
Available online at [www.jpit.az](http://www.jpit.az)17 (1)  
2026

# A conceptual framework for understanding fuzzy logic temperature controller design in electronic equipment

Rahim Mammadzada<sup>a</sup>, Kamala Aliyeva<sup>b</sup><sup>a,b</sup> Department of Instrumentation Engineering, Azerbaijan State Oil and Industry University, Azadliq Avenue str., 20, AZ1010 Baku, Azerbaijan<sup>a</sup> [rahim.mammadzada02@gmail.com](mailto:rahim.mammadzada02@gmail.com); <sup>b</sup> [kamala.aliyeva@asoiu.edu.az](mailto:kamala.aliyeva@asoiu.edu.az);

<sup>a</sup> <https://orcid.org/0009-0008-7552-2790>; <sup>b</sup> <https://orcid.org/0000-0001-5498-5982>;

## ARTICLE INFO

### Keywords:

Fuzzy logic control  
Thermal regulation  
Electronic equipment  
Conceptual framework  
Controller design  
MATLAB simulation

## ABSTRACT

Fuzzy logic control (FLC) has become a key approach for regulating temperature in modern electronic equipment, providing an adaptive and nonlinear alternative to conventional proportional–integral–derivative (PID) methods. Despite extensive studies on implementation outcomes, limited attention has been given to how engineers and learners can develop a structured understanding of the relationships between temperature dynamics, fuzzy rule construction, and controller reliability. This paper proposes a conceptual framework for understanding thermal FLC design, emphasizing the reasoning processes behind variable selection, membership function definition, and rule base construction. MATLAB-based simulation is used to illustrate how variations in these design elements influence transient and steady-state temperature behavior. By focusing on reasoning and comprehension rather than solely on implementation, the proposed framework aims to clarify the design process and support a deeper understanding of FLC thermal regulation in electronic equipment.

## 1. Introduction

Effective thermal management is essential for modern electronic systems, including computing devices, power electronics, and embedded controllers (Yusubov and Bakirova, 2023). Excessive heat can degrade component reliability, reduce efficiency, and accelerate failure, making accurate temperature regulation critical for long-term performance (Mammadov, 2025). Conventional proportional–integral–derivative (PID) controllers are commonly applied for this purpose. However, they often struggle to maintain stability under nonlinear or time-varying thermal dynamics, which motivates the use of fuzzy logic control (FLC) (Bakirova and Yusubov, 2021).

FLC offers a rule-based, intuitive approach to handling uncertainties in thermal behavior and actuator response (Aliyeva, 2025). Many studies

have focused on accurately modeling the thermal dynamics of systems, often integrating lookup tables and empirical data to capture nonlinear conduction and convection effects while maintaining manageable simulation speed (Belman-Flores et al., 2022). These efforts provide valuable implementation insights but tend to emphasize results rather than the reasoning process behind FLC design.

In practice, engineers and students frequently encounter challenges when translating their understanding of thermal systems into the design of FLC. Selecting appropriate input variables, defining membership functions, and constructing rule bases are often guided by experience rather than a systematic process (Siddikov and Umurzakova, 2020). Moreover, actuator characteristics such as fan nonlinearities or pulse width modulation (PWM) response further

Received 24 October 2025, Received in revised form 25 November 2025, Accepted 4 December 2025

<https://doi.org/10.25045/jpit.v17.i1.02>

2077-4001/© 2026 This is an open access article under the CC BY license (<https://creativecommons.org/licenses/by/4.0/>).

complicate controller tuning, particularly under worst-case or rapidly changing thermal conditions (Sun et al., 2023).

The purpose of this work is to present a conceptual framework for understanding the design process of thermal FLC for electronic equipment. The proposed approach highlights the reasoning required to define input and output ranges, interpret actuator dynamics, and integrate convection and heat transfer effects within a FLC rule base. MATLAB-based simulations are used to demonstrate how these design decisions affect transient and steady-state temperature regulation, providing a structured way to interpret the role of FLC in thermal control applications.

The remainder of this paper is organized as follows. Section 2 presents the related literature on fuzzy logic temperature control. Section 3 describes the model development. Section 4 discusses FLC design, simulation results, and compares the performance of the controllers. Section 5 concludes the paper and outlines directions for future research.

## 2. Related work

Many existing studies focus on implementation outcomes, providing a limited explanation of the underlying reasoning that connects thermal behavior to controller structure (Rajeswari Subramaniam et al., 2023). The selection of variables, definition of membership functions, and formation of rule bases are often based on experience rather than a standardized method (Siddikov and Umurzakova, 2020). As a result, researchers and engineers find it difficult to generalize design decisions across different systems, and uncertainty remains in how FLC behaves under varying thermal conditions. This highlights a gap in the literature concerning the conceptual understanding of how FLC parameters can be systematically defined for thermal and other applications.

MATLAB provides a powerful environment for studying and simulating thermal management systems, supported by its Simulink and Simscape libraries (Mammadzada, 2025a). These tools enable the integration of thermal, electrical, and mechanical domains into a unified model, which is particularly valuable for analyzing coupled effects in electronic devices (Yusubov and Bakirova, 2021). Within the Simscape thermal library, standard components such as thermal mass, conduction, and

convection blocks represent energy storage and heat transfer processes, while controlled heat sources and flow sensors capture transient and steady-state thermal behavior. This framework allows researchers to examine both passive and active heat dissipation and to estimate key parameters such as convection coefficients or equivalent capacitances without excessive computational complexity (Mammadzada, 2025b).

The reviewed works emphasize the importance of simulation-based studies in developing control strategies for thermal systems, but the reasoning behind FLC parameter configuration is still underexplored (Belman-Flores et al., 2022).

The main contributions of this work are summarized as follows:

- A conceptual framework is proposed to clarify how FLC rules and membership functions can be configured for thermal management applications.
- The approach demonstrates how steady-state thermal analysis can guide the adjustment of FLC output parameters.
- The method is implemented using MATLAB Simulink and Simscape, illustrating a clear connection between thermal modeling and FLC design.

## 3. Proposed approach

This section presents the proposed approach. Nearly all thermal systems can be described by a first-order differential equation that expresses the balance between the heat stored within the system and the heat exchanged with its surroundings (Mammadzada, 2025c):

$$C \frac{dT}{dt} = Q_{in} - Q_{out} \quad (1)$$

Where:

- $C$  is the thermal capacitance, representing the system's ability to store heat energy;
- $T$  is the measured temperature of the controlled region;
- $Q_{in}$  is the rate of heat input from sources such as heaters or electrical components;
- $Q_{out}$  is the rate of heat loss through conduction, convection, or radiation.

In electronic equipment, the dominant source is resistive heating, produced when electric current passes through conductors and semiconductor elements. Other contributions can arise from switching losses, magnetic hysteresis in inductors,

chemical reactions in batteries, or mechanical friction in actuators. At the same time, heat removal is through conduction, convection, or radiation. Conduction transfers heat through solid materials, such as from a processor to a heat sink, while convection removes energy via air or liquid movement around heated surfaces. Radiative transfer usually plays a minor role at low temperatures but becomes relevant in high-density or enclosed systems. Thermal capacity  $C$  defines how much energy must be absorbed to produce a measurable temperature rise. It acts as a form of thermal inertia, slowing down the temperature response to rapid change. While understanding thermal capacity helps interpret the system's behavior, FLC does not rely on its precise value. Instead, the controller operates based on observed

temperature changes and their relative trends. In most applications, focusing on these trends is sufficient to guide control actions, allowing learners to understand system response without relying on exact thermal parameters.

In Table 1, the parameters used for the thermal demonstration are presented. For this, a small lithium-ion battery pack was considered as the thermal system. These values represent a simplified lumped thermal mass model, allowing direct use in Simscape controlled heat source and convective blocks. The selected parameters ensure that the dominant heat transfer interactions are captured, providing a consistent framework for applying and analyzing the FLC strategy within a sufficient thermal context.

**Table 1.** Thermal model parameters used in simulation

Parameter	Symbol	Value/Range	Description / Use in Simulation
Battery thermal capacity	$C$	720 J/K	Thermal mass of the battery
Internal resistance	$R$	0.05 $\Omega$	For resistive heating ( $I^2 R$ )
Battery current	$I$	20 A	Varies to simulate load
Chemical heat coefficient	$K_{chem}$	0.08	Fraction of the resistive heating
Exposed surface area	$A$	0.04 $m^2$	Area for convective heat transfer
Natural convection coefficient	$h_{nat}$	8 $W/(m^2 \cdot K)$	Heat transfer to ambient air
Forced convection coefficient	$h_{fan}$	52 $W/(m^2 \cdot K)$	Added if the cooling fan is on
Ambient temperature	$T_{amb}$	25 $^{\circ}C$	Surrounding air temperature

Fig. 1 illustrates the overall setup used to analyze the FLC structure. The thermal subsystem functions as the plant, while two additional subsystems handle error calculation and PWM to convection conversion. This configuration reflects the operation of most real applications. An actuator

driven by a PWM signal based on control error adjusts a physical variable to maintain stability. In this demonstration, cooling is used as the control mechanism. Such setups allow testing of both proportional–integral–derivative (PID) and FLC (Yusubov and Bakirova, 2025).

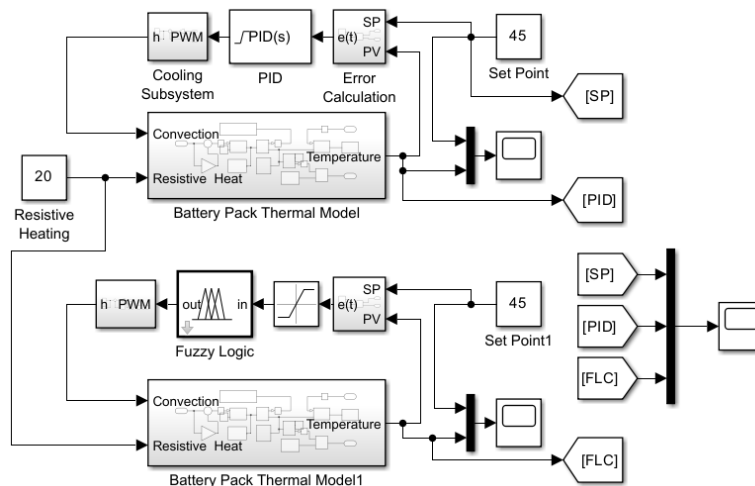


**Fig. 1.** System-level configuration with PID and FLC controllers

Fig. 2 shows the subsystem used to represent the thermal behavior of the battery. This subsystem receives the total convection coefficient and total

resistive heating, and with temperature sensor measurements, outputs the battery temperature.

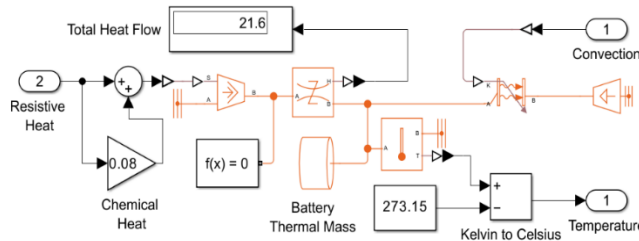


Fig. 2. Battery pack thermal subsystem

The parameters listed in Table 1 are used to configure this subsystem. The battery thermal mass is modeled with a total weight of 0.8 kg and a specific heat of 900 J/(kg·K), resulting in a heat capacity of 720 J/K. The convection block is configured with a total surface area of 0.04 m<sup>2</sup> and a variable convection coefficient, with a minimum value of 8 W/(m<sup>2</sup>·K). The total heat generation is modeled as the sum of resistive and chemical heat, where the Chemical heating is assumed to be 8% of the resistive loss, represented as a gain block with a value set to 0.08. The heat generation in a lithium-ion battery pack can be generally represented as:

$$Q_{in} = I^2R + Q_{chem} \quad (2)$$

Where:

- $I$  is the current flowing through the battery, which determines the rate of energy conversion.
- $R$  is the internal resistance of the cell, responsible for resistive (Joule) heating.
- $Q_{chem}$  is the portion of heat generated from chemical and electrochemical processes, such as side reactions and entropic effects.

Under moderate operating conditions, the chemical heating typically accounts for about 5% to 15% of the total heat produced. For demonstration or educational modeling, it can be simplified as a fixed proportion of the resistive heating, since the controller primarily responds to observable temperature variations rather than detailed internal reaction mechanisms.

$$Q_{chem} = I^2R \cdot k_{chem} \quad (3)$$

Where:

- $I^2R$  represents the resistive (Joule) heating within the cell.

- $k_{chem}$  is the proportionality factor accounting for additional chemical heat generation relative to the resistive heating.

The heat dissipation occurs inside the convection block, which utilizes the following equation.

$$Q_{out} = h_{total} \cdot A(T_{bat} - T_{amb}) \quad (4)$$

Where:

- $h_{total}$  is the total convection coefficient.
- $A$  is the total area where convection occurs.
- $T_{bat}$  is the measured battery temperature.
- $T_{amb}$  is the ambient temperature.

Fig. 3 shows the Subsystem for calculating the control error as the difference between the process variable and the setpoint, which suits cooling applications where output increases when the temperature rises above the setpoint.

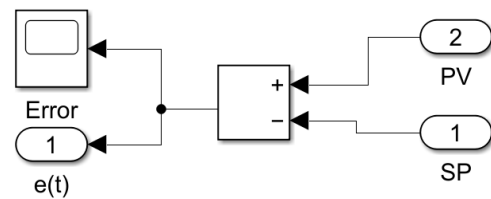


Fig. 3. Control error calculation subsystem

$$e(t) = y(t) - r(t) \quad (5)$$

Where:

- $e(t)$  is the control error.
- $y(t)$  is the process variable (PV).
- $r(t)$  is the setpoint (SP).

The control error is later passed to the corresponding controller to be analyzed and produce a PWM control signal.

Fig. 4 illustrates the subsystem responsible for adjusting the convection coefficient. To simplify the demonstration, a gain block converts the PWM signal, ranging from 0 to 1, into the corresponding forced convection for both controllers. The natural convection contribution is then added using a summation block. First-order lag is used to evade algebraic loops during simulation in Simulink.

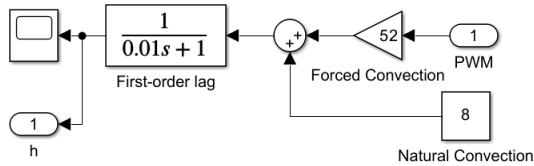


Fig. 4. Forced convection calculation subsystem

$$h_{total} = h_{nat} + h_{fan} \cdot D \tag{6}$$

Where:

- $h_{nat}$  is the natural convection 8 W/(m<sup>2</sup>·K).
- $h_{fan}$  is the forced convection 52 W/(m<sup>2</sup>·K).
- $D$  is the PWM signal.

Since the focus of this work is on the control strategy rather than exact physical implementation, the total natural convection value was set to 60 W/(m<sup>2</sup>·K). While this approach provides a reasonable approximation for fan-based cooling, actual systems often involve additional complexities, including the minimum PWM needed to initiate fan operation and the nonlinear relationship between fan speed and airflow.

#### 4. Experimental results

Apart from the modular design with subsystems, Fig. 2 also shows the controllers. The PID controller was tuned using the PID Tuner app in MATLAB, with proportional set to 0.0189, integral to 2.336, and derivative to -1.12, applying automatic tuning with saturation between 0 and 1. During tuning, the first-order lag from Fig. 4 is temporarily disconnected for plant linearization.

For the FLC, more manual configuration was required, including setting up the universe of

discourse, defining membership functions and linguistic terms, and constructing the rule base (Zadeh, 1965).

In Table 2, the input membership functions for the control error signal are listed, including their names, ranges, and universe of discourse. Three categories are defined: Negative, Zero, and Positive, spanning from -1 to 1. This setup allows the controller to determine when to engage the actuator and how strongly, with Zero representing the setpoint and the membership functions capturing the progression from initial correction to maximal adjustment as the control error increases.

Table 2. Fuzzy logic controller input variables

Name	Type	Value
Negative	Triangular fuzzy number	[-1, -1, 0.16]
Zero	Triangular fuzzy number	[-0.83, 0, 0.83]
Positive	Triangular fuzzy number	[0.16, 1, 1]

In Table 3, the initial setup for the output of the FLC control is shown. The universe is set from 0 to 1 to represent the full PWM range, with the linguistic variables spread evenly as Low at 0, Medium at 0.5, and High at 1, providing a starting point for observing and adjusting the actuator response.

Table 3. Fuzzy logic controller output variables

Name	Type	Value
Low	Real number	0
Medium	Real number	0.5
High	Real number	1

In Table 4, the FLC rule base is presented. The reasoning is straightforward. If the temperature is below the setpoint, no excessive cooling is required, but as it approaches the setpoint, the controller increases the cooling effort to maintain safe operation. The rule base is one of the simpler aspects of FLC design, as it directly reflects intuitive human reasoning and remains largely consistent across many studies in the literature.

Table 4. Fuzzy logic rule base

Number	Rule	Weight	Name
1	If the Control Error is Negative, then Cooling PWM is Low	1	Rule 1
2	If the Control Error is Zero, then Cooling PWM is Medium	1	Rule 2
3	If the Control Error is Positive, then Cooling PWM is High	1	Rule 3

Fig. 5 shows the comparison of the output signals obtained from the simulation setup. The PID controller exhibited significant overshoot, reaching nearly 52.64 °C at around step 1000, and required approximately 7000 steps to fully settle to steady state. The FLC avoided overshoot and reached a steady state of nearly 44.66 °C much faster, at around step 250. However, it exhibits a similar limitation to a PID controller with only a proportional branch, maintaining a small steady-state error. In this case, this residual error results from slightly excessive cooling rather than exceeding the 45 °C setpoint, highlighting how the FLC prioritizes safe temperature control over exact setpoint tracking. A clear understanding of how FLC parameters interact with the physical system is essential for designing a stable and responsive thermal controller. Since FLC relies on linguistic ranges rather than fixed equations, each parameter directly shapes how the controller interprets the system state and responds to temperature deviations. Without this insight, the system may either overcorrect or fail to act effectively when changes occur rapidly.

This inherent limitation of the FLC can provide insight into the trade-offs involved in its design. The FLC output operates within a normalized range of 0 to 1, corresponding directly to the PWM signal’s minimum and maximum duty cycle. A value of 0 signifies no active cooling, only natural convection, while 1 represents full actuator output for maximum forced cooling. One of the most important parts of the FLC is the midpoint value of

the output membership functions, which defines the steady-state condition. This can be set through trial and error or determined analytically by examining the thermal system under steady-state conditions, where the generated heat equals the dissipated heat (Mammadzada, 2025b).

$$\frac{dQ_{gen}}{dt} = \frac{dQ_{conv}}{dt} \tag{7}$$

Where:

- $\frac{dQ_{gen}}{dt}$  is the total instantaneous heat generation.
- $\frac{dQ_{conv}}{dt}$  is the total instantaneous heat dissipation.

Although in real applications, calculating this ideal condition is rarely possible, FLC offers an effective way to approximate it through qualitative reasoning rather than precise mathematical modeling. However, understanding this ideal scenario first helps establish the reasoning behind the equations used in this study. From here, by subsuming the equations for both heat generation and convection, we get:

$$I^2R + Q_{chem} = h_{ss} \cdot A(T_{bat} - T_{amb}) \tag{8}$$

Where:

- $h_{ss}$  is the convection coefficient required to reach the steady-state condition.

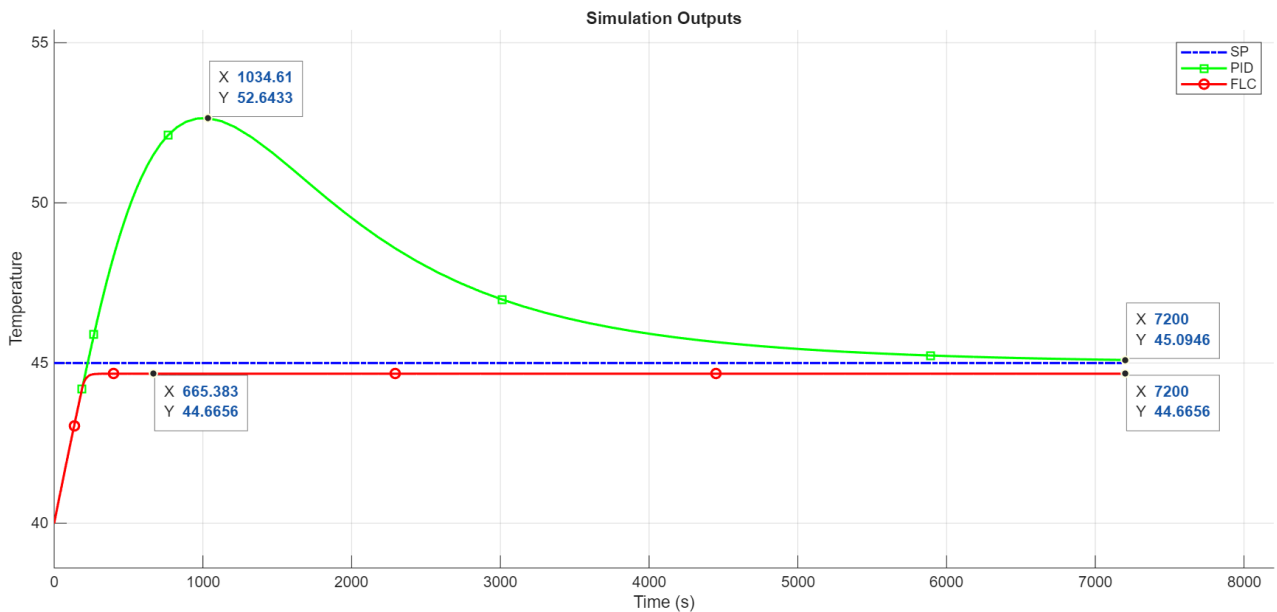


Fig. 5. Temperature Comparison between FLC and PID Controllers

From here, we can calculate the convection coefficient required for a steady-state condition as:

$$h_{ss} = \frac{I^2 R + Q_{chem}}{A(T_{bat} - T_{amb})} \quad (9)$$

From here, by substituting the predefined values from Table 2, including the input heat generation of 21.6 W, total convection area of 0.04 m<sup>2</sup>, steady-state battery temperature of 45 °C, and ambient temperature of 25 °C, the resulting steady-state convection coefficient is calculated as 27 W/(m<sup>2</sup>·K). Using this value, the required PWM signal can then be determined based on the difference between the total and natural convection coefficients, divided by the effective range of forced convection.

$$D = \frac{h_{ss} - h_{nat}}{h_{total} - h_{nat}} \quad (10)$$

In Table 5, the updated rule base for the steady-state adjusted FLC is presented, where the calculated PWM value is assigned to the “Medium” output level. In this configuration, the PWM signal required to maintain the setpoint D is calculated as 0.3653, serving as a practical reference for defining the controller’s balanced operating condition between minimal and maximal cooling effort.

Fig. 6 shows the temperature response of the system for both the initial Table 3 (FLC1) and the steady-state adjusted Table 5 (FLC2). In the first

setup, where the output midpoint was set to 0.5, the controller maintained the temperature slightly below the setpoint, leading to a noticeable steady-state error. After adjusting the midpoint to 0.3653 based on steady-state thermal analysis, the adjusted controller (FLC2) reached the setpoint with much higher precision but stabilized longer.

**Table 5.** Steady-state adjusted FLC output values

Name	Type	Value
Low	Real number	0
Medium	Real number	0.3653
High	Real number	1

Fig. 7 shows the PWM control signals generated by both controllers. The initial case (FLC1) applied stronger actuation across the simulation (PWM1), while the adjusted version (FLC2) used a smoother and more efficient response (PWM2) to achieve a better cooling effect.

Although in this idealized case the FLC successfully reached the near-exact setpoint, real applications rarely achieve such precision. Pure FLC inherently involve trade-offs, and changes in input heat generation can cause either overshoot or steady-state error even in an adjusted design. However, this model can serve as a worst-case scenario estimate, helping to refine the input ranges by understanding how and when the controller should begin reacting to deviations.

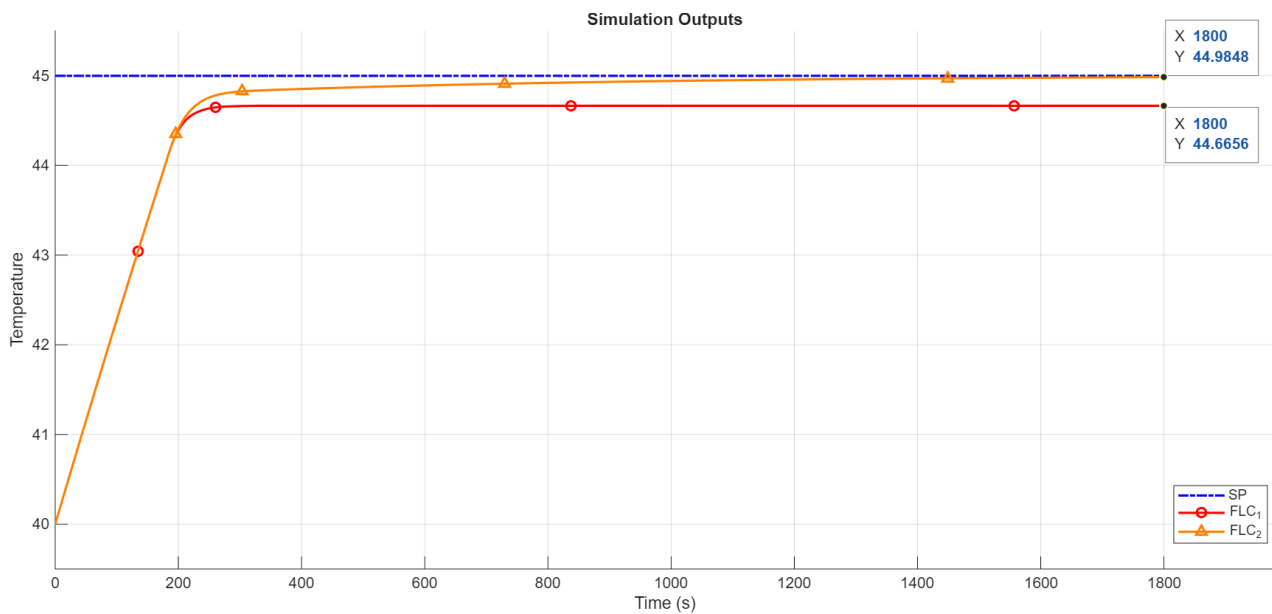


**Fig. 6.** Temperature comparison between initial and tuned FLC responses

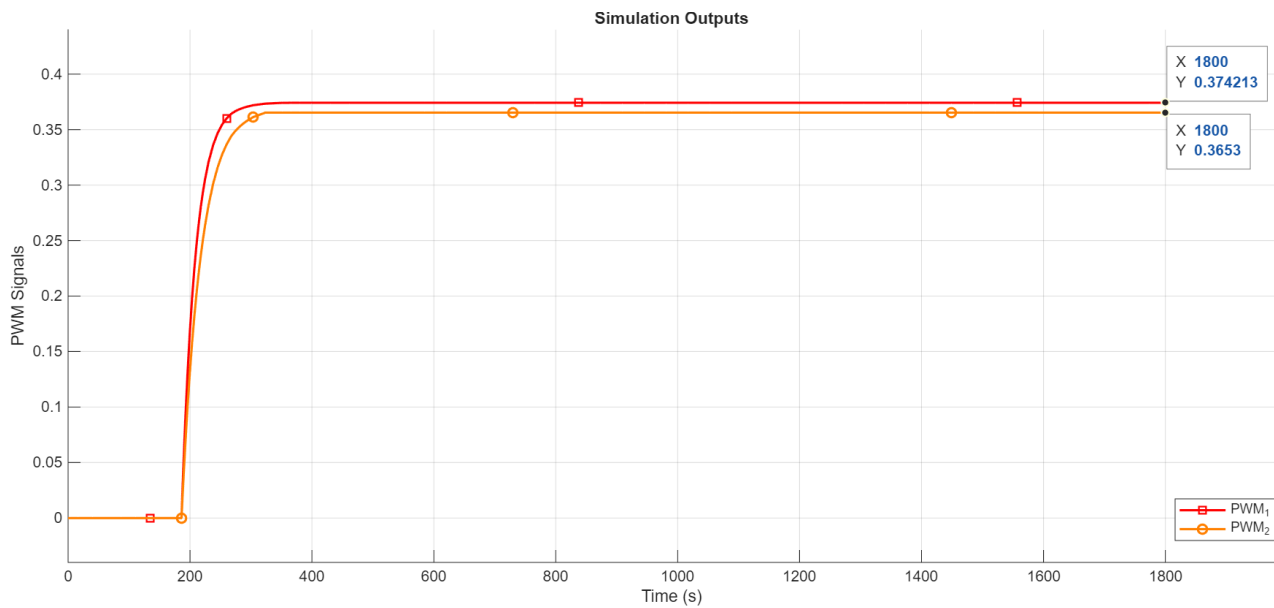


Fig. 7. PWM signal comparison between initial and tuned FLCs

For the input, defined as the control error, the sign of this error determines the system's position relative to the setpoint and how the controller should respond. Adjusting the lower and upper limits of the input affects the controller's response range, determining when corrective actions begin and when maximum actuation is reached. Properly defining these boundaries helps ensure that the controller reacts proportionally to thermal deviations while maintaining stability.

For the Negative control error (below zero), when the measured temperature is below the setpoint. Cooling should remain minimal, allowing natural heating or internal system losses to bring the control error closer to zero. The lower limit should consider the system's thermal inertia, ensuring that cooling does not begin prematurely.

For the Zero control error (around zero), when the system is near or at the desired setpoint. The controller output should stabilize around the midpoint, balancing heat generation and dissipation to maintain steady-state operation. Small fluctuations are expected and can be tolerated without excessive actuation.

For the Positive control error (above zero), when the setpoint has been exceeded, it indicates that stronger cooling is required. The upper limit should be defined by the acceptable deviation before performance or safety is affected, while also accounting for actuator capacity and response time to avoid over-correction or oscillations.

Additional parameters, such as a greater number of membership functions or the inclusion of the rate of error change as a second input, can further refine control within these regions.

However, the fundamental understanding of fuzzy thermal regulation is built upon how effectively the controller manages the error itself.

## 5. Conclusion and future work

Although a pure FLC cannot achieve perfect precision at every point, it effectively models human-like reasoning to deliver stable, adaptive temperature control. By analyzing the thermal system, designers can estimate worst-case conditions and tune the controller's input and output ranges accordingly. The upper input limit determines when maximum corrective effort is required, the lower limit defines when control begins, and the output midpoint reflects the steady-state balance between heat generation and dissipation. This structured approach enables smooth transitions and prevents excessive cooling or overheating under varying loads.

Despite the presence of steady-state error due to its qualitative nature, FLC transforms system understanding into practical decision rules that remain intuitive and transparent. It enhances interpretability compared to purely mathematical methods, revealing the sensitivity of parameters and the trade-offs between responsiveness and stability.

Integrating FLC with conventional PID control combines adaptive reasoning with precise tuning. This hybrid approach ensures accurate setpoint regulation while maintaining smooth and effective thermal management for diverse electronic applications. This perspective offers insight that may inform future FLC design frameworks.

## References

- Aliyeva, K. (2025). Estimation of renewable energy sources under uncertainty using fuzzy AHP method. *Informatyka, Automatyka, Pomiary w Gospodarce i Ochronie Środowiska*, 15(2), 104-109. <https://doi.org/10.35784/iapgos.7191>
- Bakirova, L., & Yusubov, E. (2021). Design and Simulation of the Auto-Tuning TS-Fuzzy PID Controller for the DC-DC ZETA Converter. In *CEUR Workshop Proceedings* (pp. 238-243). <https://elibrary.ru/item.asp?id=49020698>
- Belman-Flores, J. M., Rodríguez-Valderrama, D. A., Ledesma, S., García-Pabón, J. J., Hernández, D., & Pardo-Cely, D. M. (2022). A review on applications of fuzzy logic control for refrigeration systems. *Applied Sciences*, 12(3), 1302. <https://doi.org/10.3390/app12031302>
- Mammadov, R. (2025, July). Optimal Load Shedding for Power Systems Using the Binary Exhaustive Search Method. In *International Conference on Intelligent and Fuzzy Systems* (pp. 175-183). Cham: Springer Nature Switzerland. [https://doi.org/10.1007/978-3-031-98304-7\\_20](https://doi.org/10.1007/978-3-031-98304-7_20)
- Mammadzada, R. (2025a). Design of a fuzzy set-point tracking controller based on the state-dependent control characteristics of fuzzy logic and PID for temperature control systems in electrical equipment. *Chemical Technology, Control and Management*, 2025(6), Article 8. <https://doi.org/10.59048/2181-1105.1746>
- Mammadzada, R. (2025b). Performance evaluation of PID and fuzzy logic control strategies under charge-discharge cycles in a Simscape-based thermal-electrical battery system. *Journal of Modern Technology and Engineering*, 10(3), 213-223. <https://doi.org/10.62476/jmte.103213>
- Mammadzada, R. (2025c). System-level conceptual analysis of thermal behavior in solar microgrids with fuzzy logic perspective. *Journal of Modern Technology and Engineering*, 10(3), 141-148. <https://doi.org/10.62476/jmte.103141>
- Rajeswari Subramaniam, K., Cheng, C. T., & Pang, T. Y. (2023). Fuzzy logic controlled simulation in regulating thermal comfort and indoor air quality using a vehicle heating, ventilation, and air-conditioning system. *Sensors*, 23(3), 1395. <https://doi.org/10.3390/s23031395>
- Sun, W., Si, H., Li, Y., Wang, H., Qiu, J., & Li, G. (2023). Fuzzy Control Algorithm Applied on Constant Airflow Controlling of Fans. *Energies*, 16(11), 4425. <https://doi.org/10.3390/en16114425>
- Yusubov, E., & Bakirova, L. (2021, September). A Self-Tuning Fuzzy PID Controller for SEPIC Based on Takagi-Sugeno Inference System. In *2021 International Conference Automatics and Informatics (ICAI)* (pp. 54-57). IEEE. <https://doi.org/10.1109/ICAI52893.2021.9639804>
- Yusubov, E., & Bekirova, L. (2023). The optimized power flow control system for the photovoltaic DC microgrid. In *E3S Web of Conferences* (Vol. 404, p. 03001). EDP Sciences. <https://doi.org/10.1051/e3sconf/202340403001>
- Yusubov, E., & Bekirova, L. (2025). Stability of metaheuristic PID controllers in photovoltaic dc microgrids. *Informatyka, Automatyka, Pomiary w Gospodarce i Ochronie Środowiska*, 15. <https://doi.org/10.35784/iapgos.6410>
- Siddikov, I. X., & Umurzakova, D. M. (2020). Fuzzy-logical control models of nonlinear dynamic objects. *Advances in Science, Technology and Engineering Systems*, 5(4), 419-423. <http://dx.doi.org/10.25046/aj050449>
- Zadeh, L. A. (1965). Fuzzy sets. *Information and control*, 8(3), 338-353. [https://doi.org/10.1016/S0019-9958\(65\)90241-X](https://doi.org/10.1016/S0019-9958(65)90241-X)